Cancer Immunology, Immunotherapy (2021) 70:2937–2950
https://doi.org/10.1007/s00262-021-02894-8

ORIGINAL ARTICLE

Polymorphism of formyl peptide receptor 1 (FPR1) reduces the therapeutic efficiency and antitumor immunity after neoadjuvant chemoradiotherapy (CCRT) treatment in locally advanced rectal cancer

Shu-Fen Chiang[1,2] · Kevin Chih-Yang Huang[3,4] · William Tzu-Liang Chen[5] · Tsung-Wei Chen[6,7] · Tao-Wei Ke[8] · K. S. Clifford Chao[2]

Received: 27 August 2020 / Accepted: 15 February 2021 / Published online: 13 March 2021

Abstract

Immunosurveillance and immunoscavenging prompted by preoperative chemoradiotherapy (CCRT) may contribute to improve local control and increase survival outcomes for patients with locally advanced rectal cancer (LARC). In this study, we investigated several genotypes of pattern recognition receptors (PRRs) and their impact on therapeutic efficacy in LARC patients treated with CCRT. We found that homozygosis of formyl peptide receptor 1 (FPR1) (E346A/rs867228) was associated with reduced 5-year overall survival (OS) by Kaplan–Meier analysis (62% vs. 81%, $p=0.014$) and multivariate analysis [hazard ratio (HR) = 3.383, 95% CI = 1.374–10.239, $p=0.007$]. Moreover, in an animal model, we discovered that the FPR1 antagonist, Boc-MLF (Boc-1), reduced CCRT therapeutic efficacy and decreased cytotoxic T cells and T effector memory cells after chemoradiotherapy treatment. Pharmacologic inhibition of FPR1 by Boc-1 decreased T lymphocyte migration to irradiated tumor cells. Therefore, these results revealed that the FPR1 genotype participates in CCRT-elicited anticancer immunity by reducing T lymphocytes migration and infiltration, and that the FPR1-E346A CC genotype can be considered an independent biomarker for chemo- and radiotherapy outcomes.

Keywords FPR1 · CCRT · ICD · DAMP · Cancer immunity

Abbreviations

5-fluorouraci	5-FU
CCRT	Concurrent chemoradiotherapy
CRC	Colorectal cancer
DAMP	Danger-associated molecular pattern
DFS	Disease-free survival
FPR1	Formyl peptide receptor 1
GzmB	Granzyme B
ICD	Immunogenic cell death
LARC	Locally advanced rectal cancer patients
LOF	Loss of function
OS	Overall survival
P2RX7	P2X purinergic receptor 7
PRR	Pattern recognition receptors
SNPs	Single nucleotide polymorphisms
TRG	Tumor regression grade
TILs	Tumor-infiltrating lymphocytes

Tao-Wei Ke and K. S. Clifford Chao contributed equally to this work.

✉ Tao-Wei Ke
d18047@mail.cmuh.org.tw

✉ K. S. Clifford Chao
d94032@mail.cmuh.org.tw

[1] Laboratory of Precision Medicine, Ministry of Health & Welfare Feng Yuan Hospital, Taichung 42055, Taiwan

[2] Cancer Center, China Medical University Hospital, China Medical University, Taichung 40402, Taiwan

[3] Department of Biomedical Imaging and Radiological Science, China Medical University, Taichung 40402, Taiwan

[4] Translation Research Core, China Medical University Hospital, China Medical University, Taichung 40402, Taiwan

[5] Department of Colorectal Surgery, Hsinchu China Medical University Hospital, Hsinchu 40402, Taiwan

[6] Department of Pathology, China Medical University Hospital, China Medical University, Taichung 40402, Taiwan

[7] Graduate Institute of Biomedical Science, China Medical University, Taichung 40402, Taiwan

[8] Department of Colorectal Surgery, China Medical University Hospital, China Medical University, Taichung 40402, Taiwan

Introduction

Colorectal cancer (CRC) is one of the leading causes of death worldwide [1], and ~ 30% of CRC cases are rectal cancer [2]. In locally advanced rectal cancer patients (LARC), concurrent chemoradiotherapy (CCRT) followed by total mesorectal excision surgery is considered the most effective strategy and standard treatment to improve local control, better survival, and functional preservation of the sphincter [3, 4]. CCRT is the combination of radiotherapy and fluorouracil-based chemotherapy [5]. After CCRT, the pathologic response is assessed by tumor regression grade (TRG) on surgery specimen, and approximately 40–60% patients achieved some degree of tumor regression [6, 7]. However, even in complete tumor regression, which greatly decreases the risk of locoregional recurrence, the late development of distant metastasis is still a major cause of mortality in LARC [8, 9].

In addition to direct damage to tumor cells, cytotoxic agents and radiotherapy induce immunosurveillance and immunoscavenging, enhancing anticancer immune responses to control tumor growth. Many studies have reported that recruitment of TILs within the tumor microenvironment (TME) is associated with the therapeutic efficacy of chemoradiotherapy and correlates with improved relapse-free and overall survival in patients with CRC [10–12]. Chemotherapy and radiotherapy causes danger-associated molecular pattern (DAMP) release from dying cancer cells to induce immunogenic cell death (ICD), which then initiates the immune response, triggers dendritic cell maturation, activates adaptive antitumor responses and recruits tumor-infiltrating lymphocytes (TILs) [13–15]. Hence, the release of these DAMPs and subsequent perception by pattern recognition receptors (PRRs) on immune cells are important processes to initiate a series of events involved in antitumor immune responses.

These DAMPs interact with various immune cells by PRRs to prime and launch antitumor immunity. For example, ATP release attracts DC recruitment via P2X purinergic receptor 7 (P2RX7), calreticulin exposure triggers DC uptake via CD91, and HMGB1 release activates the tumor antigen presentation process via TLR4 or TIM3 receptor [16–18]. Annexin A1 (ANXA1) is a novel DAMP that is associated with the therapeutic response to chemotherapy, especially anthracycline-based drugs such as mitoxantrone and doxorubicin. The ANXA1 receptor formyl peptide receptor 1 (FPR1) belongs to the PRRs and plays a key regulatory role in innate immunity. In addition, FPR is mostly expressed on DC progenitor and myeloid cells and mediates neutrophil activation, DC positioning and maturation, and antitumor immunity [19, 20]. Lack of FPR1 or blocking with the FPR1 antagonist cyclosporin H (CsH) abolished chemotherapy efficacy in breast cancer because these dendritic cells are incapable of getting close to dead cancer cells for cross-presentation of tumor-associated antigens to cytotoxic T lymphocytes, suggesting that the interaction between ANXA1 and FPR1 is important for the antitumor immune response [19, 21].

Recently, several nonsynonymous single nucleotide polymorphisms (SNPs) of PRRs have been reported to influence the therapeutic responses to chemotherapy. For instance, TLR1-S602I (rs5743618) is associated with the survival outcome of FOLFIRI plus bevacizumab treatment in metastatic CRC patients [22]. A loss of function (LOF) SNP of FPR1-E346A (rs867228, c. 1037 A > C, p.Glu346Ala, where Ala is the LOF allele), was reported to have a negative impact on patients with breast cancer receiving anthracycline or oxaliplatin treatment [23, 24]. However, no information regarding these SNPs on PRRs is available to evaluate the therapeutic efficacy of preoperative CCRT on LARC patients.

In this study, we investigated several germline polymorphisms of PRRs that have putative alterations of receptor function, including TIM3 (R140L/rs1036199), P2RX7 (E496A/rs3751143), TLR1 (S602I/rs5743618) and FPR1 (E346A/rs867228), to evaluate their clinical significance and impact on survival outcome after CCRT treatment in LARC patients.

Materials and methods

Patient characteristics, clinical staging, treatment, and pathological evaluation

From 2006 to 2014, 211 patients with LARC were treated at China Medical University Hospital (CMUH). Among these patients, 171 received CCRT followed by surgery. Finally, 130 patients with biopsy-proven LARC available surgical tissue, and cT3-4 or cN + were included in this study cohort. These patients completed preoperative chemoradiotherapy, and radical resection was performed after 6–8 weeks as previously described [25]. Resected specimen pathologic staging was based on the American Joint Committee on Cancer (AJCC) staging system, and clinical stage based on EUS, MRI or CT and the percentage was 7.7%, 13.1% and 79.2%, respectively. Biopsy and resected specimens were reviewed by pathologists, and their clinical response was assessed after the completion of CCRT according to rigorous criteria involving clinical, endoscopic, and radiologic findings. Pathologic complete response (pCR) was defined and scored by tumor regression grade (TRG) as previously described [6, 25]. Adjuvant chemotherapy regimens were administered as previously described [5, 14]. This study was reviewed and approved by the Institutional Review Board (IRB) of CMUH [Protocol number: CMUH105-REC2-072].

Genomic DNA extraction and SNP genotyping

Genomic DNA from non-tumor tissues of rectal cancer patients was extracted from two 5 µm thick FFPE slides using a QIAamp® DNA FFPE Extraction Kit (QIAGEN GmbH, Hilden, Germany). For SNP genotyping, 10 ng of total genomic DNA was used for PCR amplification and was performed using the iPLEX® HS panel on the MassARRAY® System (Agena Bioscience, San Diego, CA, USA), which employs matrix-assisted laser desorption/ionization time-of-flight mass spectrometry for amplicon detection (MALDI-TOF-MS; SpectroACQUIRE, Agena Bioscience). Primers designed (Supplementary Table 1) for PCR amplification of specific polymorphisms and extension reactions were prepared using MassARRAY® Assay Design Version 3.1 software (Agena Bioscience, San Diego, CA, USA). Following PCR, SAP addition, and the iPLEX HS® extension reaction, the samples were desalted by resin treatment for 15 min, spotted onto SpectroCHIP® Arrays (Agena Bioscience, San Diego, CA), analyzed by mass spectrometry, and ultimately interpreted using SpectroTYPER v4.0 software (Agena Bioscience, San Diego, CA).

Tissue microarrays immunohistochemistry (IHC)

Tissue microarrays were constructed from pair-matched pre-CCRT biopsies and post-CCRT surgical tissue from LARC patients and IHC was performed using 3 µm sections as previously described [14, 26, 27]. The following antibodies were used in this study: anti-human $CD8^+$ (1:100, ab4055, Abcam, Cambridge, UK). The stained tissue array sections were scored separately by two pathologists blinded to the clinicopathological parameters. $CD8^+$ TILs (no. of TILs/high-power field) were evaluated at 400 × magnification by two pathologists as our previously study described [25]. The average number of $CD8^+$ TILs in five high-power fields was included in the evaluation: A count of zero in a high-power field was given a score of 0, a count of 1–3 was given a score of 1, a count of 4–10 was given a score of 2, and a count of > 10 was given a score of 3.

Administration of tumor-bearing mice with concurrent chemoradiotherapy (CCRT) and FPR1 blockade

BALB/c mice (female, 4 weeks old) were maintained in specific pathogen-free conditions according to the institutional guidelines approved by the China Medical University Institutional Animal Care and Use Committee. Four-week-old female wild-type BALB/c mice were obtained from BioLASCO Taiwan Co (Taipei, Taiwan) and accommodated for 1 week for the following experiments. CT26 cells (5×10^5 cells/mouse) were suspended in 100 µl of 50% Matrigel matrix (mixed with PBS) and injected subcutaneously into the left leg of each mouse. Animals were randomly assigned to three groups receiving or not receiving two cycles of the CCRT regimen [5-FU (5-fluorouraci) (5 mg/kg, intraperitoneal injection) and 5 Gy on the left legs of mice] in combination or not in combination with 25 mg/kg i.p. Boc-1 (Enzo Life Biosciences, Lausen, Switzerland) as described in Fig. 2a. The tumor volume, body weight and survival time were measured every 2–3 days, and mice were sacrificed on day 19. The tumor volumes were calculated according to the formula ($\text{width}^2 \times \text{length}$)/2. The mice were sacrificed at the termination of the experiments, and the tumor tissues from representative mice were collected for immunohistochemistry analysis.

Immunofluorescent staining

All samples were fixed in 10% neutral buffered formalin and embedded in paraffin, were cut with 4 µm, deparaffin and rehydrated using routine protocols. Antigen retrieval was performed with citrate-based antigen unmasking solution (H3300, Vector Lab, CA, USA) and then used 5% goat serum for blocking. Anti-granzyme B antibody (1:100, ab4059, Abcam, Cambridge, UK) incubation was performed overnight at 4 °C and Alexa 488-conjugated anti-rabbit secondary antibody was performed at room temperature for 1 h. The slide was then incubated with anti-CD8a antibody (1:100, ab209775, Abcam, Cambridge, UK) overnight at 4 °C, and Alexa 546-conjugated anti-rabbit secondary antibody was performed at room temperature for 1 h. Finally, the slides were counterstain with Hoechst 33,342 Fluorescence Stain (Thermo Scientific, Massachusetts, USA) and were mounted with Vector shield fluorescence mounting medium (Vector Labs, CA, USA).

Isolation of tumor-infiltrating lymphocytes (TILs) for FACS analysis

BALB/c experimental mice were sacrificed at day 19 after tumor inoculation. Tumor was isolated and weighted from the mice, and then placed in petri dish containing blank RPMI media at room temperature to keep it in media to prevent dehydration. Tumor was minced into small pieces (1–2 mm) by beaver blade and filtered through a 70-µm strainer, spun down, and then resuspended in blank RPMI media. Thereafter, the cell suspensions were layered over Ficoll-Paque media, centrifuged at 1,025 g for 20 min, transfer the layer of mononuclear cells into a conical tube and added 20 ml with complete RPMI media, and then gently mix and centrifuge at 650 g for 10 min for twice. Finally, removed the supernatant and resuspended the TILs with complete RPMI media.

Then, TILs were resuspended in 500-µL staining buffer (2% BSA, 0.1% NaN_3 in PBS). The cells were stained with a surface marker panel, containing CD8a (551,162, BD PharMingen, CA, USA), CD44 (E-AB-F1100C, Elabscience, Texas, USA), CD45 (E-AB-F1136D, Elabscience, Texas, USA) and their isotype, A PE Rat IgG2b, κ isotype control was included for CD45, FITC Rat IgG2b (E-AB-F09842D, Elabscience, Texas, USA), a FITC Rat IgG2b, κ Isotype Control was for CD44 (E-AB-F09842C, Elabscience, Texas, USA). Samples were analyzed on the Novocyte 3000 Flow Cytometer analyzer (ACEA bio, CA, USA). Finally, % of TILs/tumor weight (%/g) was calculated from the percentage of each subtype in TILs by gating CD45+ cells and adjusted with the weight of each tumor.

Immature DC and T lymphocyte culture and fluorescence labeling

Human monocytic leukemia cell line THP-1 and human T cell leukemia Jurkat cell lines were purchased from BCRC (Hsinchu, Taiwan). Cells were cultured and maintained in RPMI1640 medium supplemented with 10% FCS (Life Technologies, Grand Island, New York, USA), 2 mM glutamine, 1 mM sodium pyruvate, 100 U/ml penicillin, and 100 mg/ml streptomycin at 37 °C in a humidified incubator with 95% air and 5% CO_2. Immature DC was generated from THP-1 as previously described [28]. Briefly, THP-1 cells were differentiated to immature DC by adding with 1500 IU/ml rhIL-4 (Sino Biological, Beijing, China) and 1500 IU/ml rhGM-CSF (Sino Biological, Beijing, China) in culture medium for at least 7 days, with cytokine-supplemented culture medium changed every 2–3 days at 37 °C in a humidified incubator with 95% air and 5% CO_2. For fluorescence labeling to detect cells migration, THP-1-derived immature DCs and T lymphocytes were labeled with CellTracker™ Red CMTPX (Invitrogen, CA, USA) and CFSE (Invitrogen, CA, USA) according to the manufacturer's instructions, respectively. Briefly, the cells were harvested by centrifugation and incubated in serum-free medium with 10 µM CellTracker™ Red CMTPX or 5 µM CFSE at 37 °C for 30 min and then washed with culture medium three times.

Determine the effect of Boc-1 on immature DC and T lymphocyte migration by irradiated tumor cells in vitro

Irradiated human colorectal cancer cell lines HCT-116 cells were co-cultured with fluorescence-labeled THP-1-derived immature DCs and Jurkat T lymphocytes using a Transwell system. Briefly, HCT-116 cells (1×10^5) were seeded and cultured into 24-well 0.4-µm pore size Transwell plate (Corning, CA, USA) for overnight, and then exposed to 10 Gy radiation. After 16–18 h incubation, CMTPX-labeled immature DCs (1×10^5) and CFSE-labeled T lymphocytes (2×10^5) were added into 5-µm pore size inserts on the plate and co-cultured for 24 h with or without 20 µM Boc-1. Finally, the lower wells were fixed with 4% paraformaldehyde for 15 min at room temperature and then observed using inverted fluorescence microscopy (Zeiss, Germany). The cell number of immature DCs and T lymphocytes migration was imaged and quantified with five random fields of each well (AxioVision 4.91 software; Zeiss).

Knockdown FPR1 expression and immunoblotting

For knockdown experiments, FPR1 was silenced with 25 nM of siRNA duplex (sense: GUCAGAAUCCGUGAGUUAU, antisense: AUAACUCACGGAUUCUGAC). A negative control siRNA was used with no significant sequence similarity to human gene sequences. Briefly, the cells were transfected with siRNA using Lipofectamine 3000 (ThermoFisher Scientific, Paisley, Scotland), according to the manufacturer's instructions. After 18 h, the transfection medium was replaced with a complete medium, and the cells were collected for experiments and analyzed by immunoblotting. The cell lysates (30 µg) were quantified and separated by 10% sodium dodecyl sulfate polyacrylamide gel electrophoresis, and then transferred onto a PVDF membrane (GE, Amersham, UK). The membranes were blocked with 5% non-fat milk, incubated with FPR1 antibodies (1:1000, Abcam, MA, USA) overnight at 4 °C, horseradish peroxidase (HRP)-conjugated secondary antibodies (1:10,000, GE Healthcare, Amersham, UK) and followed by the immobilon western chemiluminescent HRP substrate (Millipore, MA, USA) for detection. Finally, the results of western blots were detected by the AlphaImager2200 digital imaging system (Digital Imaging System, CA, USA) and analyzed by ImageJ software (NIH, MD, USA) [25].

Statistical analysis

JMP statistical software version Pro 12 (SAS Institute, NC, USA) was used to perform the statistical analyses. All tests reported a two-sided p value with a significance level set at 0.05. Student's t test, Pearson chi-square test and Fisher's exact test were used for group comparisons. Cox regression analysis was used to estimate the hazard ratios (HRs) and 95% confidence intervals (CIs) for univariate and multivariate models. Influential factors that affected the rectal cancer patient survival rate were adjusted in the Cox models. Weibull parametric model was used for estimating the 5-year OS and DFS probability. The univariate comparison was performed using the log-rank test.

Results

Clinical characteristics and genotype of PRRs in LARC patients

We designed several primers to identify immune-related candidate genetic defects associated with therapeutic responses to chemoradiotherapy. These genetic polymorphisms of PRRs, namely, TIM3 (R140L/rs1036199), P2RX7 (E496A/rs3751143), TLR1 (S602I/rs5743618) and FPR1 (E346A/rs867228), are nonsynonymous single nucleotide polymorphisms (SNPs). DNA was extracted and genotyped from adjacent normal tissues of rectal cancer patients, surgery specimens after CCRT treated ($n = 130$). The individual genotypes and allele frequencies were shown and consistent with the global allele frequencies in Table S2, which was classified based on the NCBI dbSNP and ClinVar database. The genotype TT of TIM3 (rs1036199), AA of P2RX7 (rs3751143), TT of TLR1 (rs5743618) and CC of FPR1 (rs867228) were prevalent among LARC patients.

Table 1 presents the clinicopathological characteristics and genotype group of TIM3, P2RX7, TLR1, and FPR1 within the LARC patients ($n = 130$). The median radiation dose was 50.4 Gy administered in 28 fractions (minimum dose: 44.8 Gy; maximum dose: 50.4 Gy). Concurrent chemotherapy was infusional 5-fluorouracil in 9% of patients, UFT in 39% of patients, and capecitabine in 44% of patients. The mean age at diagnosis was 59.7 ± 12.6 years (range, 31–90 years). The majority of the patients were men (67%). The surgical specimens were reviewed and scored based on the Tumor Regression Grade (TRG) system [7]. After CCRT treatment following by surgery, only 13 patients (10%) presented a pathologic complete response (TRG 4, no residual tumor), and 13 patients (10%) also presented a clinical complete response, while 47 patients (36%) presented with lymph node metastases. Moreover, 55 patients (43%) exhibited distant metastasis within 10 years.

In the SNP genotype analysis, the recessive model was used to classify these SNP genotypes. No correlation was observed between clinicopathological parameters and P2RX7-E496A or TLR1-S602I genotype. LOF CC genotype of FPR1-E346A was significantly correlated with clinical stage, chemotherapy, and $CD8^+$ TILs.

The CC Genotype of FPR1-E346A is significantly associated with survival outcome, TRG, and $CD8^+$ TILs in LARC

The estimated 5-year disease-free survival (DFS, the time to cancer recurrence or death after diagnosis) and overall survival (OS) rates of CCRT-treated LARC patients were 63% and 59%, respectively (Table 2). The median follow up was 67.8 months (3.2 to 141.5 months). Among the clinicopathological parameters, we found that the pT stage, pN stage, clinical response, TRG, histological grade, lymphovascular invasion (LVI), perineural invasion (PNI) and pre-CCRT $CD8^+$ TILs were remarkably associated with 5-year DFS and OS after CCRT treatment in LARC patients (Table 2). Among the 4 genetic polymorphisms of PRRs, only the CC genotype of FPR1-E346A was markedly associated with a worse 5-year overall survival (OS) by Kaplan–Meier survival analysis (Fig. 1). Furthermore, we analyzed the correlation between these clinicopathological parameters and FPR1 genotype by odds ratio. Poor TRG and low $CD8^+$ TILs in the pre-CCRT group were significantly associated with patients carrying CC genotype of FPR1-E346A. The odds ratios were 2.521 (95% CI = 1.163–5.473, $p = 0.017$) and 2.294 (95% CI = 1.036–5.076, $p = 0.039$), respectively (Table 2). These results suggested that the FPR1-E346A CC genotype was associated with shortened overall survival, less $CD8^+$ TILs in the tumor microenvironment, and poor pathologic response of LARC patients with CCRT treatment.

Prognostic impact of the FPR1 polymorphism on LARC patients who received CCRT treatment

As shown in Table 3, the pT3-4 stage, positive pN stage, poor clinical response, poor TRG, poor differentiation, presence of lymphovascular invasion (LVI), presence of perineural invasion (PNI), and low pre-CCRT $CD8^+$ TILs exhibited a significantly higher risk in 5-year DFS and 5-year OS by univariate analysis. Only FPR1-E346A CC genotype had a notably higher risk in 5-year OS among the 4 PRRs.

Subsequently, we examined these parameters by multivariate Cox regression analysis to clarify the independent prognostic factors for LARC patients who received CCRT treatment. Our results showed that PNI (HR = 2.163, 95% CI = 1.027–4.668, $p = 0.042$) was an independent prognostic factor of 5-year DFS. FPR1-E346A CC genotype (HR = 3.383, 95% CI = 1.364–10.239, $p = 0.007$) was an independent prognostic factor of 5-year OS for LARC patients (Table 3). These data strongly indicated that the FPR1-E346A polymorphism has significant prognostic value for LARC patients following CCRT treatment.

Pharmacologic blockade of FPR1 signaling markedly led to tumor growth after concurrent chemoradiotherapy in vivo

To further validate that the therapeutic efficacy of concurrent chemoradiotherapy (CCRT) was modulated by FRP1 signaling to trigger antitumor immunity, we used Boc-MLF

Table 1 Clinicopathological parameters and genotypes of PRRs in this study

Clinicopathological parameters	Total cases (%)	TIM3 (R140L/rs1036199)			P2RX7 (E496A/rs3751143)			TLR1(S602I/rs5743618)			FPR1 (E346A/rs867228)		
		GG + GT	TT	*p* value	AA + AC	CC	*p* value	GG + GT	TT	*p* value	AA + AC	CC	*p* value
	130 (100%)	21(16%)	109 (84%)		124(95%)	6 (5%)		23 (18%)	107 (82%)		55 (43%)	73 (57%)	
Age				0.103			0.404			0.163			0.056
< 65	86 (66%)	17 (81%)	69 (63%)		83 (67%)	3 (50%)		18 (78%)	68 64%)		31 (56%)	53 (73%)	
≥ 65	44 (34%)	4 (19%)	40(37%)		41 (33%)	3 (50%)		5 (22%)	39 (36%)		24 (44%)	20 (27%)	
Sex				0.045*			0.381			0.105			0.986
Female	43 (33%)	11 (52%)	32 (29%)		40 (32%)	3 (50%)		11 (48%)	32 (30%)		18 (33%)	24 (33%)	
Male	87 (67%)	10 (48%)	77 (71%)		84 (68%)	3 (50%)		12(52%)	75 (70%)		37 (67%)	49 (67%)	
Histological grade				0.619			0.357			0.895			0.643
Well	6	1 (5%)	5 (5%)		6 (5%)	6 (100%)		1 (4%)	5 (5%)		1 (1.8%)	4 (5%)	
Moderate	100	18 (85%)	82 (75%)		94 (76%)	0 (0%)		19 (83%)	81 (75%)		42 (76%)	57 (78%)	
Poor	8	1 (5%)	7 (6%)		8 (6%)	0 (0%)		1 (4%)	7 (7%)		4 (7%)	4 (5%)	
Unknown	16	1 (5%)	15 (14%)		16 (13%)	0 (0%)		2 (9%)	14 (13%)		8 (15%)	8 (11%)	
TMN stage (7^{th} AJCC)				0.147			0.129			0.133			0.033*
I	5 (4%)	1 (1%)	4 (4%)		5 (24%)	1 (17%)		0 (00%)	5 (5%)		1 (2%)	4 (5%)	
II	50 (38%)	10 (53%)	40 (36%)		33 (27%)	3 (50%)		10 (44%)	40 (37%)		21 (38%)	28 (39%)	
III	69 (53%)	8 (42%)	61 (55%)		40 (36%)	2 (33%)		12 (52%)	57 (53%)		33 (60%)	35 (48%)	
IV	6 (5%)	0 (0%)	6 (5%)		5 (4%)	0 (0%)		1 (4%)	5 (5%)		0 (0%)	6 (8%)	
pN stage				0.768			0.882			0.744			0.658
Negative	83 (64%)	14 (67%)	69 (63%)		79 (64%)	4 (67%)		14 (61%)	69 (64%)		36 (66%)	45 (62%)	
Positive	47 (36%)	7 (33%)	40 (37%)		45 (36%)	2 (33%)		9 (39%)	38 (36%)		19 (34%)	28 (38%)	
TRG				0.157			0.204			0.178			0.093
4	13 (10%)	1 (5%)	12 (11%)		13 (10%)	0 (0%)		1 (4%)	12 (11%)		6 (11%)	7 (10%)	
3	71 (55%)	11 (52%)	60 (55%)		68 (55%)	3 (50%)		13 (57%)	58 (54%)		36 (65%)	34 (46%)	
2	29 (22%)	8 (38%)	21 (19%)		26 (21%)	3 (50%)		8 (35%)	21 (20%)		7 (13%)	21 (29%)	
1	17 (13%)	1 (5%)	16 (15%)		17 (14%)	0 (0%)		1 (4%)	15 (15%)		6 (11%)	11 (15%)	
Clinical response				0.768			0.23			0.949			0.579
Complete response	13 (10%)	1 (5%)	12 (11%)		13 (11%)	0 (0%)		2 (9%)	11 (10%)		6 (11%)	7 (10%)	
Partial response	48 (37%)	9 (43%)	39 (36%)		47 (38%)	1 (17%)		8 (34%)	40 (37%)		18 (33%)	28 (38%)	
Stable disease	61 (47%)	10 (47%)	51 (47%)		56 (45%)	5 (83%)		11 (48%)	50 (47%)		29 (52%)	32 (44%)	
Progression disease	8 (6%)	1 (5%)	7 (6%)		8 (6%)	0 (0%)		2 (9%)	6 (6%)		2 (4%)	6 (8%)	
Concurrent chemotherapy				0.816			0.402			0.589			0.024*
Capecitabine	57 (44%)	8 (38%)	49 (45%)		53 (43%)	4 (66%)		8 (35%)	49 (46%)		23 (42%)	32 (44%)	
UFT	51 (39%)	10 (48%)	41 (38%)		50 (40%)	1 (17%)		11 (48%)	40 (38%)		25 (46%)	26 (36%)	
5-FU	12 (9%)	2 (10%)	10 (9%)		11 (9%)	1 (17%)		3 (13%)	9 (8%)		7 (13%)	5 (7%)	
Others	10 (8%)	1 (5%)	9 (8%)		10 (8%)	0 (0%)		1 (4%)	9 (8%)		0 (0%)	10 (14%)	
Lymphovascular invasion (LVI)				0.565			0.248			0.792			0.162

Table 1 (continued)

Clinicopathological parameters	Total cases (%)	TIM3 (R140L/rs1036199)			P2RX7 (E496A/rs3751143)			TLR1(S602I/rs5743618)			FPR1 (E346A/rs867228)		
		GG + GT	TT	*p* value	AA + AC	CC	*p* value	GG + GT	TT	*p* value	AA + AC	CC	*p* value
Absent	99 (76%)	17 (81%)	82 (75%)		95 (77%)	4 (67%)		18 (78%)	81 (76%)		45 (82%)	52 (71%)	
Present	31 (24%)	4 (19%)	27 (25%)		29 (23%)	2 (33%)		5 (220%)	26 (24%)		10 (18%)	21 (29%)	
Perineural invasion (PNI)				0.853			0.723			0.679			0.106
Absent	95 (73%)	15 (71%)	80 (73%)		91 (73%)	4 (67%)		16 (70%)	79 (74%)		44 (80%)	49 (67%)	
Present	35 (27%)	6 (29%)	29 (27%)		33 (27%)	2 (33%)		7 (30%)	28 (26%)		11 (20%)	24 (33%)	
Distance metastasis				0.358			0.645			0.197			0.093
No	73 (57%)	14 (67%)	61 (56%)		71 (57%)	4 (67%)		16(70%)	59 (55%)		36 (65%)	37 (51%)	
Yes	55 (43%)	7 (33%)	48 (44%)		53 (43%)	2 (33%)		7 (30%)	48 (45%)		19 (35%)	36 (49%)	
pre-CCRT $CD8^+$ TILs				0.267			0.293			0.397			0.039*
Low	86 (70%)	16 (80%)	70 (68%)		83 (71%)	3 (50%)		17 (77%)	69 (68%)		30 (60%)	55 (77%)	
High	37 (30%)	4 (20%)	33 (32%)		34 (29%)	3 (50%)		5 (23%)	32 (32%)		20 (40%)	16 (23%)	
NA	7	1	6		7	0		7	6		5	2	

pN stage: positive (Stage 1a + 1b + 2) Versus negative (Stage 0); $CD8^+$ TILs: high (grade 2 + 3) Versus low (grade 0 + 1); Chi-squared test was used. Fisher's exact test was used when > 25% of the cells had expected counts < 5. NA: not available. The contrast test did not include the "NA" group

(Boc-1), a mouse FPR1 antagonist, to mimic the loss of function of FPR1-E346A. The concurrent chemoradiotherapy regimen and Boc-1 treatment on BALB/c mice is described in Fig. 2a. We found that tumor volume was dramatically reduced in mice receiving CCRT (Fig. 2b). However, with Boc-1 treatment, the regression of tumor volume was markedly reduced compared to those mice that received CCRT only (Fig. 2b). Similarly, the resected tumor showed that tumor weight was significantly increased in the CCRT/Boc-1 group on day 19 compared to the mice that received CCRT only (Fig. 2c). To further examine antitumor immunity and the phenotype of T cells within the TME, the status of T cells within resected tumor were evaluated by flow cytometry including $CD8a^+$ cytotoxic T cells and $CD8a^+$ $CD44^+$ effector memory T cells [29–31]. We found that CCRT remarkably enhanced the density of $CD8a^+$ T cells or $CD8a^+$ $CD44^+$ T cells infiltration. But the infiltration of $CD8a^+$ T cells and $CD8a^+$ $CD44^+$ T cells was significantly decreased in CCRT/Boc-1-treated group (Fig. 2d, e). Moreover, the activated T cells $CD8a^+$ and granzyme B (GzmB) within resected tumors was examined by immunofluorescent stain. We found that CCRT significantly promoted the number of $CD8a^+$ and $CD8a^+$ $GzmB^+$ TILs in the central tumor region. But the number of $CD8a^+$ and $CD8a^+$ $GzmB^+$ TILs was also remarkably reduced in CCRT/Boc-1-treated mice (Fig. 2f, h). These results indicated that FPR1 may participate for chemoradiotherapy-induced lymphocyte infiltration and affects the therapeutic efficacy of CCRT, especially cytotoxic and effector memory T cells. Taken together, these results showed the FPR1 signaling pathway may be important for chemoradiotherapy-induced antitumor immunity.

FPR1 inhibition decreased T lymphocyte migration to irradiated tumor cells in vitro

Previous studies have demonstrated that radiotherapy-induced release of DAMPs, such as HMGB1 contributes to enhance anti-tumor immunity by increasing recruitment and maturation of immune cells, especially dendritic cells [32]. To determine the influence of Boc-1 on immature DC and T lymphocytes, we analyzed whether THP-1-derived immature DCs (THP1-iDCs) and Jurkat T lymphocytes can be attracted by irradiated HCT116 cells. HCT116 cells were seeded on the lower chamber of a Transwell and irradiated with 10 Gy radiation. After overnight incubation, the CMTPX–labeled THP1-iDCs and CSFE-labeled Jurkat T lymphocytes were seeded on the upper wells. After 24 h incubation with or without 20 μM Boc-1, the migration ability of THP1-iDCs and Jurkat T lymphocytes (upper well) toward irradiated HCT116 cells (lower well) was analyzed. We found that the Boc-1 did not affect the migration of THP1-iDC (Fig. 3a), but significantly reduced the recruitment of Jurkat T lymphocytes (Fig. 3b). Moreover, in the THP1-iDCs and Jurkat

Table 2 The relationship between clinicopathologic parameters, PRRs genotype and 5-year DFS and OS

Clinicopathologic parameter	Total case	5-year DFS %	*p* value	5-year OS %	*p* value	FPR1 CC genotype (E346A/rs867228)	
						Odd ratio (95% CI)	*p* value
	130	63%		59%			
Age			0.822		0.142		0.0559
≥65	44	65%		62%		0.487 (0.232–1.022)	
<65	86	63%		74%		1	
Sex			0.656		0.025*		0.986
Female	43	66%		83%		0.993 (0.471–2.093)	
Male	87	62%		64%		1	
pT stage			0.0003*		0.0001		0.9
T3-4	76	50%		58%		1.046 (0.5123–2.132)	
T0-2	54	83%		87%		1	
pN stage			< 0.0001*		0.0003*		0.658
Positive	47	38%		52%		1.179 (0.568–2.443)	
Negative	83	78%		80%		1	
Histological grade			0.006*		< 0.0001*		0.634
Poor	8	20%		5%		1.419 (0.336–5.986)	
Moderate to well	106	64%		71%		1	
Unknown	16						
Clinical response			0.006*		0.018*		0.628
Poor response	69	52%		61%		1.190 (0.589–2.404)	
Good response	61	76%		68%		1	
TRG			0.029*		0.0001*		0.017*
Poor response	46	52%		31%		2.521 (1.162–5.473)	
Good response	84	70%		80%		1	
Lymphovascular invasion (LVI)			< 0.0001*		< 0.0001*		0.162
Present	31	31%		37%		1.817 (0.775–4.261)	
Absent	99	74%		80%		1	
Perineural invasion (PNI)			<0.0001*		0.0009*		0.102
Present	35	29%		50%		1.959 (0.861–4.455)	
Absent	95	76%		77%		1	
pre-CCRT $CD8^+$ TILs			0.005*		0.007*		
Low	86	58%		65%		2.294 (1.036–5.076)	0.039*
High	37	86%		88%		1	
NA	7						
post-CCRT $CD8^+$ TILs			0.194		0.542		
Low	73	61%		69%		1.396 (0.614–3.171)	0.423
High	38	75%		76%		1	
NA	19						
TIM3 SNP (R140L/rs1036199)			0.669		0.361		0.271
TT	109	63%		81%		0.565 (0.2–1.596)	
GG + GT	21	62%		67%		1	
P2RX7 SNP (E496A/rs3751143)			0.383		0.782		0.143
GG	6	83%		63%		0.569(0.268–1.211)	
AA + AG	124	62%		70%		1	
TLR1 SNP (S602I/rs5743618)			0.757		0.241		0.377
TT	107	62%		67%		0.658(0.257–1.685)	
GG + GT	23	69%		82%		1	
FPR1 SNP (E346A/rs867228)			0.178		0.014*		–
CC	73	58%		62%		–	
AA + AC	55	69%		81%		–	

pN stage: positive (Stage 1a + 1b + 2) Versus negative (Stage 0); Clinical response: Good response (complete response and partial response) Versus Poor response (stable disease and progression disease); TRG: Good response (TRG 3–4) Versus Poor response (TRG 1–2); $CD8^+$ TILs: high (grade 2 + 3) Versus low (grade 0 + 1); Weibull parametric model was used for estimating survival probability, and *p* value was obtained from log-rank test. Logistic regression was used for the odd ratio and 95% confidence interval (CI), and *p* value was obtained from Pearson's chi-square test. NA: not available. The contrast test did not include the "NA" group

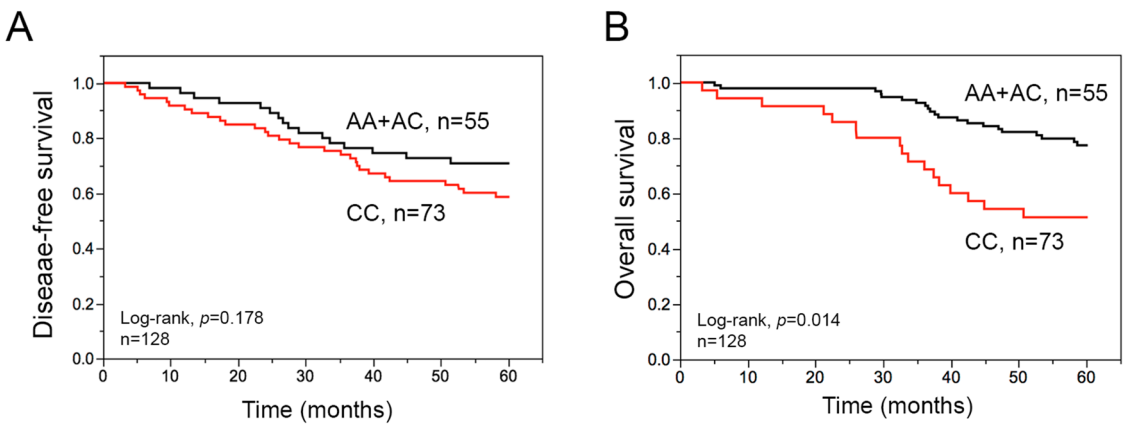

Fig. 1 The association between disease-free survival (DFS), overall survival (OS) and FPR1 genotypes in LARC **a** Kaplan–Meier curve showed that the FPR1-E348A CC genotype is associated with 10-year DFS. **b** Kaplan–Meier curve showed that the FPR1-E348A CC genotype is associated with 10-year OS

Table 3 Univariate and multivariate of PRRs genotype and clinicopathological parameters in 5-year DFS and OS

Variable	No. at Risk	Disease-free survival			Overall survival		
		HR	95% CI	*p* value	HR	95% CI	*p* value
Univariate							
Age (≥65 vs < 65)	130	0.932	0.489–1.697	0.823	1.612	0.832–3.045	0.152
Sex (Male vs Female)	130	1.153	0.628–2.231	0.652	2.479	1.157–6.131	0.018*
pT stage (T3-4 vs T1-2)	130	3.558	1.796–7.860	0.0001*	3.829	1.786–9.473	0.0003*
pN stage (Positive vs Negative)	130	3.476	1.933–6.412	< 0.0001*	3.116	1.642–6.044	0.0005*
Histological grade (Poor vs Moderate to well)	114	3.176	1.199–7.039	0.023*	5.792	2.296–12.786	0.0006*
Clinical response (Poor response vs Good response)	130	2.367	1.288–4.578	0.005*	2.239	1.154–4.603	0.017*
TRG (Poor response vs Good response)	130	1.884	1.050–3.367	0.034*	3.551	1.868–6.956	0.0001*
Lymphovascular invasion (Present vs absent)	130	3.522	1.948–6.304	< 0.0001*	4.411	2.314–8.407	< 0.0001*
Perineural invasion (Present vs absent)	130	4.333	2.415–7.813	< 0.0001*	2.836	1.475–5.373	0.002*
TIM3-R140L genotype (TT vs GG + GT)	130	0.983	0.467–2.404	0.968	1.615	0.642–5.412	0.335
P2RX7-E496A genotype (GG vs AA + AG)	130	0.852	0.432–1.580	0.621	1.223	0.198–4.001	0.788
TLR1-S602 genotype (TT vs GG + GT)	130	1.135	0.541–2.774	0.754	1.842	0.733–6.177	0.210
FPR1-E346A genotype (CC vs AA + AC)	128	1.513	0.836–2.845	0.173	2.407	1.208–5.212	0.012*
pre-CCRT $CD8^+$ TILs (Low vs High)	123	3.539	1.518–10.317	0.002*	3.805	1.501–12.814	0.003*
Multivariate							
pT stage (T3-4 vs T1-2)	106	2.670	0.793–9.004	0.111	3.165	0.919–11.512	0.067
pN stage (Positive vs Negative)	106	1.688	0.772–3.755	0.189	1.983	0.841–4.773	0.117
Histological grade (Poor vs Moderate to well)	106	1.313	0.362–3.816	0.648	1.931	0.603–5.305	0.247
Clinical response (Poor response vs Good response)	106	1.518	0.519–3.094	0.425	1.914	0.643–5.099	0.230
TRG (Poor response vs Good response)	106	1.239	0.355–1.864	0.611	2.340	0.943–5.887	0.066
Lymphovascular invasion (Present vs absent)	106	1.083	0.472–2.451	0.847	1.586	0.663–3.788	0.297
Perineural invasion (Present vs absent)	106	2.163	1.027–4.668	0.042*	1.056	0.499–2.250	0.884
FPR1-E346A genotype (CC vs AA + AC)	106	1.657	0.785–3.755	0.189	3.383	1.364–10.239	0.007*
pre-CCRT $CD8^+$ TILs (Low vs High)	106	2.456	0.929–8.468	0.071	2.376	0.791–10.241	0.131

T lymphocytes co-culture, we observed that THP1-iDC were surrounded by Jurkat T lymphocytes in the lower chamber in the control group, but this phenomenon was found to a lesser extent in the Boc-1-treated group (Fig. 3c). These data indicated that Boc-1 affects T cell recruitment toward irradiated HCT116 cells. For realizing the impact of FPR1 expression on the migration ability of THP1-iDC and Jurkat T lymphocytes, we transient transfected siRNA carrying

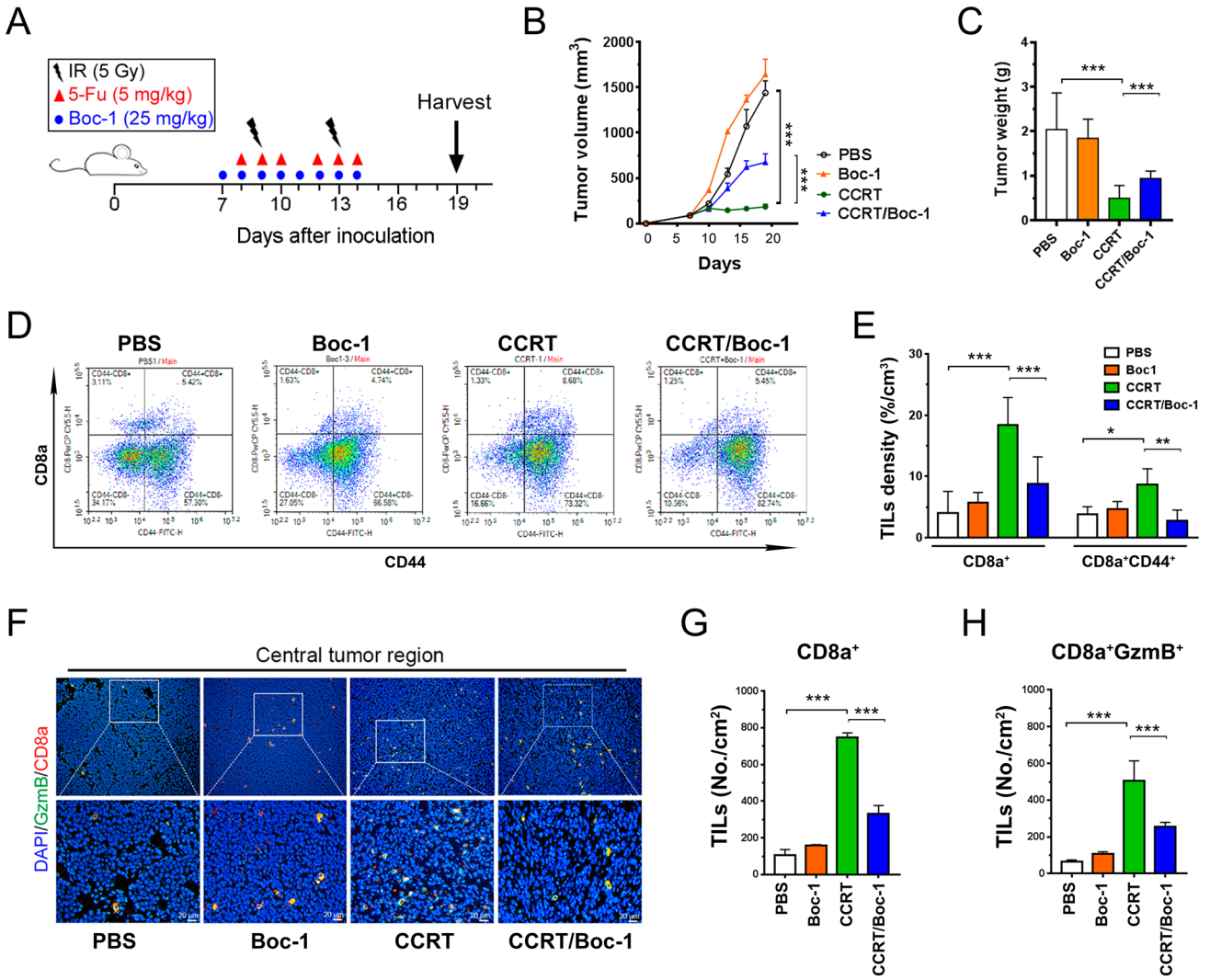

Fig. 2 FPR1 signaling is required for TIL infiltration and antitumor immunity in vivo. **a** The graphic scheme of the concurrent chemoradiotherapy regimen on BALB/c mice. **b** Tumor growth of CT26-driven colon carcinoma established in BALB/c mice ($n=5$ per group) that were treated with concurrent chemoradiotherapy [CCRT, 5-FU (5 mg/kg) and 5 Gy for 2 fractions or CCRT/Boc-1 (25 mg/kg FPR inhibitor one hour before 5-FU). Tumor growth is calculated as the mean tumor volume ± SD over time. ***$p<0.001$. ANOVA test. **c** Resected tumors were extracted and examined ($n=5$). ***p < 0.001. ANOVA test. **d** TILs were isolated from resected tumors and analyzed by flow cytometry. Dot plot of $CD8a^+$ and $CD44^+$ TILs was based on the gating of $CD45^+$ cells. **e** Statistical analyses of $CD8a^+$ and $CD8a^+$ $CD44^+$ TILs density in resected tumors ($n=3$ per group). The density (%/cm^3) was calculated by percentage of the cells and adjusted by each tumor weight, which 1 g tumor is approximately 1 cm3. ***$p<0.001$, **$p<0.01$, *$p<0.05$. ANOVA test. **f** Immunofluorescence stain with $CD8a^+$ and granzyme B in the central tumor region. **g** and **h** The number of $CD8a^+$ or $CD8a^+$/granzyme B TILs was counted under high-power-field microscopy ($n=5$). ***$p<0.001$. ANOVA test

negative control (NC) and siFPR1 into THP1-iDC and Jurkat T lymphocytes, we found that both THP1-iDC and Jurkat cell expressed FPR1. The knockdown efficiency of siFPR is ~ 50–70% (Fig. 3d). Moreover, knockdown of FPR1 significantly inhibited the migration ability in both THP1-iDC and Jurkat T lymphocytes (Fig. 3e, f). These results suggested that FRP1 was expressed on immature DC and T lymphocytes to regulate cells migration. Hence, FPR1 may participate in CCRT-induced DC and T cell infiltration.

Discussion

In this study, we verified that loss of function of FPR1-E346A by homozygosis was associated with shortened OS and DFS, decreased $CD8^+$ effector T cell infiltration and attenuated therapeutic efficacy of CCRT treatment. Furthermore, we examined the role of FPR1 in antitumor immunity during concurrent chemoradiotherapy treatment in vivo. We found that pharmacological inhibition of FPR1 by Boc-1 dramatically reduced the therapeutic efficacy of CCRT and

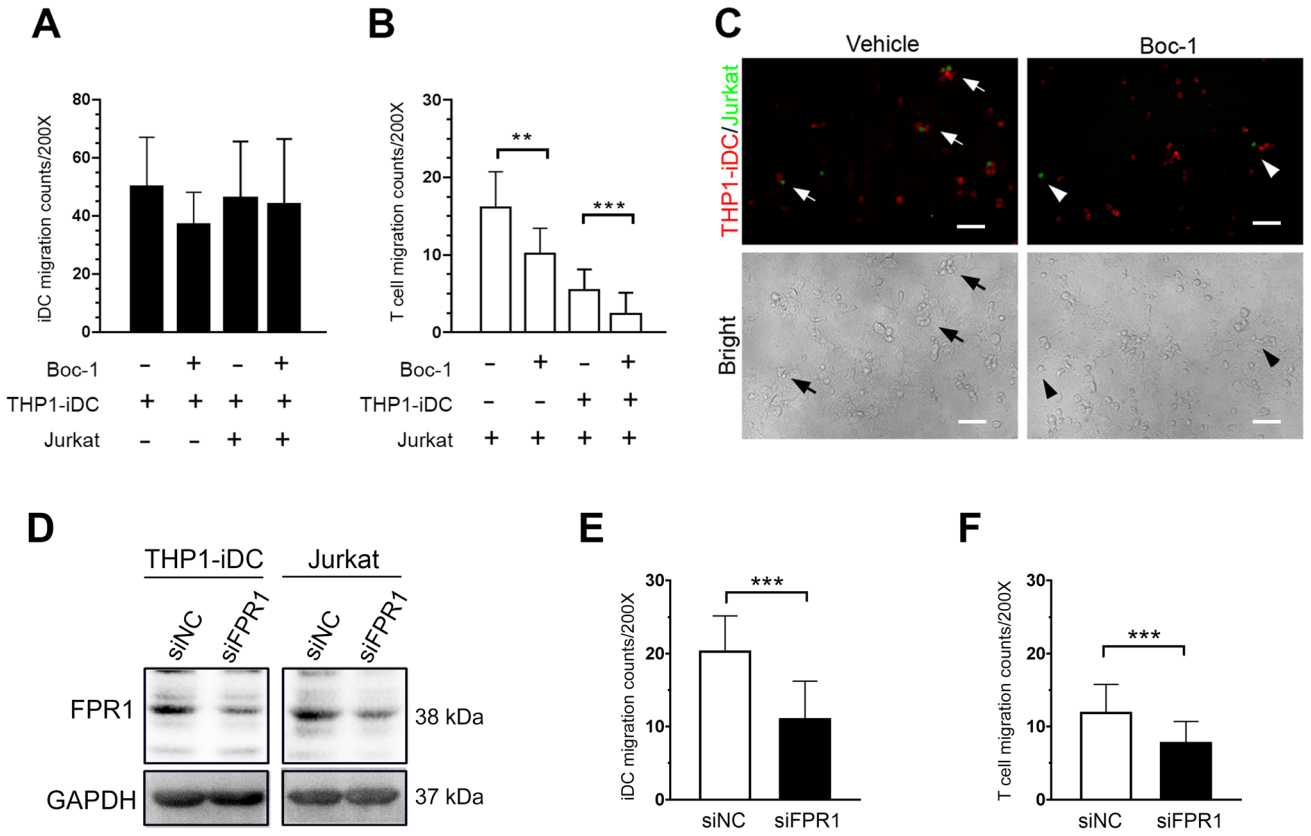

Fig. 3 FPR1 blockade affects T cells recruitment and closed contact formation with DCs in vitro.HCT116 cells were seeded and irradiated (10 Gy) on the lower well of Transwell for overnight culture. The CMTPX–labeled (Red) THP1-iDCs and/or CSFE-labeled (Green) Jurkat T lymphocytes were seeded on the upper wells for 24 h incubation. **a** The number of migrated THP1-iDCs into irradiated HCT116 cells with or without 20 μM Boc-1 treated ($n=5$). Unpaired t test. **b** The number of migrated Jurkat T cells into irradiated HCT116 cells with or without 20 μM Boc-1 treated ($n=5$). $^{**}p<0.01$ and $^{***}p<0.001$. Unpaired t test. These data were obtained from at least three independent experiments. The values represent the means ± S.D. **c** The closed contact between THP-1-derived immature DCs and Jurkat T lymphocytes within irradiated HCT116 cells (200X). Scale bars = 20 μm. **d** Immunoblotting analysis of FPR1 expression. THP1-iDCs and Jurkat T lymphocytes were transfected with siRNA against negative control (NC) and FPR1. **e** The number of THP1-iDCs-siNC, THP1-iDCs-siFPR1, Jurkat-siNC and Jurkat-siFRP1 migrated into irradiated HCT116 cells ($n=3$). $^{***}p<0.001$. Unpaired t test. The values represent the means ± S.D

decreased the recruitment of cytotoxic and effector/memory T lymphocytes in vivo and inhibited T cell migration to irradiated tumor cells in vitro. Hence, blockade of FPR1 may influence the therapeutic efficacy of radiotherapy by suppressing anticancer immunity.

Several studies have demonstrated that FPR1 is necessary for chemotherapy-induced antitumor immunity. Blockade of FPR1 attenuated chemotherapy efficacy in breast cancer [21, 33]. FPR1-E346A was also reported to have a negative impact on anthracycline or oxaliplatin treatment in patients with breast cancer and colorectal cancer [24, 34]. In our clinical results, we found that FPR1-E346A in homozygosis is associated with a worse DFS and OS after CCRT, and these results indicated that FPR1-E346A reduced the anticancer efficacy of CCRT. In addition, in an in vivo study, we used Boc-1 to block mouse FPR1 function before and during CCRT treatment and found that CCRT together with Boc-1 did not effectively inhibit tumor growth compared to CCRT treatment alone. Blocking FPR1 function significantly reduced the therapeutic efficacy of CCRT. Our findings indicated that the function of FPR1 can be considered an independent factor for therapeutic outcome for CCRT-treated LARC patients.

Regarding antitumor immunity, radiotherapy is a more effective strategy than chemotherapy because radiation triggers more immune responses by DAMPs and sometimes has abscopal effects on non-irradiated tumors. Hence, radiation is considered as in situ vaccination by inducing ICD, exposing DAMPs, recruiting myeloid cells, and priming T lymphocytes [32, 35]. Similarly, CCRT is a powerful therapeutic strategy, which enhances adaptive immunity. Therefore, CCRT creates an ideal in situ tumor vaccination

microenvironment for reinvigorating the immune system to achieve systemic tumor regression and abscopal effects.

The expression of FPR1 has been reported to be important for the differentiation of monocytes to dendritic cells and macrophages and the recruitment of neutrophils [36, 37]. FPR1 is a G-protein-coupled receptor (GPCR) and E346 is located at the extreme C-terminus of FPR1. E346A exchange largely reduces the constitutive activity of FPR by altering the interaction with G_i-proteins and is considered as a loss of function substitution and causes defective signal transduction [38]. Vacchelli et al. proved that FPR1-deficient DCs did not lose their recruitment ability toward chemotherapy-treated dying cancer cells, but failed to approach and establish stable contact with dying cancer cells to elicit antitumor T cell immunity [24]. Moreover, Lee et al. found that FPR1 is expressed in cytosol and/ or nucleus on T cells and triggered surface expression and migration by agonist stimulation, but decreased migration on FPR1-knockdown of naïve $CD4^+$ T cells [39]. Our results confirmed either blockade of FPR1 by Boc-1 or FPR1-knockdown could decrease T cells migration toward irradiated tumor cells in vitro. Consistently, the results of our animal study showed that blockade of FPR1 obviously decreased $CD8a^+$ TILs infiltration within the tumor microenvironment and reduced tumor regression after CCRT treatment in vivo, especially cytotoxic and effector/memory T cells. Our clinical study also showed that the loss of function FPR1-E346A was correlated with less $CD8^+$ TILs and worse survival outcome after CCRT treatment. Therefore, deficiency of FPR1 function may affect T cells migration toward dying tumor cells, and decrease the infiltration of cytotoxic and effector/memory T cells into tumor. Hence, we believe that FPR1-E346A may lead to insufficient T cell-mediated antitumor immunity and attenuate the immunosurveillance and immunoscavenging ability, and finally affect the therapeutic efficacy of CCRT.

Based on the present results, we demonstrate that the FPR1 polymorphism participates in CCRT-elicited antitumor immunity and can be considered an independent biomarker of therapeutic outcome. Functional FPR1 may be a key point for achieving an effective anticancer immune response. Unfortunately, over 50% of patients with LARC carried the FPR1-E346A variant and displayed poor prognosis with CCRT treatment. Hence, FPR1 genotype evaluation may help in stratifying and improving the therapeutic efficacy of CCRT in LARC patients.

Supplementary Information The online version contains supplementary material available at https://doi.org/10.1007/s00262-021-02894-8.

Authors contribution Shu-Fen Chiang and Kevin Chih-Yang Huang conducted and performed the experiments; Tao-Wei Ke, William Tzu-Liang Chen and Tsung-Wei Chen enrolled the LARC patients and performed IHC evaluation; Shu-Fen Chiang performed the statistical analysis; Shu-Fen Chiang and K. S. Clifford Chao supervised this study; Shu-Fen Chiang, Kevin Chih-Yang Huang, and K. S. Clifford Chao analyzed the data and wrote the manuscript. All authors read and approved the final manuscript version.

Funding This study was supported by grants from China Medical University Hospital (DMR-108-221), the Ministry of Science and Technology (MOST106-2314-B-039-005), the Ministry of Science and Technology (MOST107-2314-B-039-027-MY3 and MOST107-2314-B-039-057-MY3, Taiwan), and the Health and welfare surcharge of tobacco products, China Medical University Hospital Cancer Research Center of Excellence (MOHW109-TDU-B-212-134024, Taiwan).

Compliance with ethical standards

Conflict of interest The authors have declared that no conflicts of interest exist.

Ethical approval All subjects gave their informed consent for inclusion before they participated in the study. The study was conducted in accordance with the Declaration of Helsinki, and the protocol was approved by the Institutional Review Board (IRB) of CMUH [Protocol number: CMUH105-REC2-072].

Human and animal rights All experimental work has been conducted in accordance with relevant national legislation on the use of animals for research by Affidavit of Approval of Animal Use Protocol China Medical University (CMUIACUC-2018-015).

References

1. Siegel RL, Miller KD, Jemal A (2017) Cancer statistics, 2017. CA Cancer J Clin 67(1):7–30. https://doi.org/10.3322/caac.21387
2. Conde-Muino R, Cuadros M, Zambudio N, Segura-Jimenez I, Cano C, Palma P (2015) Predictive biomarkers to chemoradiation in locally advanced rectal cancer. Biomed Res Int 2015:921435. https://doi.org/10.1155/2015/921435
3. Sauer R, Liersch T, Merkel S, Fietkau R, Hohenberger W, Hess C, Becker H, Raab HR, Villanueva MT, Witzigmann H, Wittekind C, Beissbarth T, Rodel C (2012) Preoperative versus postoperative chemoradiotherapy for locally advanced rectal cancer: results of the German CAO/ARO/AIO-94 randomized phase III trial after a median follow-up of 11 years. J Clin Oncol 30(16):1926–1933. https://doi.org/10.1200/JCO.2011.40.1836
4. Sauer R, Becker H, Hohenberger W, Rodel C, Wittekind C, Fietkau R, Martus P, Tschmelitsch J, Hager E, Hess CF, Karstens JH, Liersch T, Schmidberger H, Raab R, German Rectal Cancer Study G (2004) Preoperative versus postoperative chemoradiotherapy for rectal cancer. N Engl J Med 351 (17):1731–1740. https://doi.org/10.1056/NEJMoa040694
5. Yoon WH, Kim HJ, Kim CH, Joo JK, Kim YJ, Kim HR (2015) Oncologic impact of pathologic response on clinical outcome after preoperative chemoradiotherapy in locally advanced rectal cancer. Ann Surg Treat Res 88(1):15–20. https://doi.org/10.4174/astr.2015.88.1.15
6. Losi L, Luppi G, Gavioli M, Iachetta F, Bertolini F, D'Amico R, Jovic G, Bertoni F, Falchi AM, Conte PF (2006) Prognostic value of Dworak grade of regression (GR) in patients with rectal carcinoma treated with preoperative radiochemotherapy. Int J Colorectal Dis 21(7):645–651. https://doi.org/10.1007/s00384-005-0061-x

7. Dworak O, Keilholz L, Hoffmann A (1997) Pathological features of rectal cancer after preoperative radiochemotherapy. Int J Colorectal Dis 12(1):19–23. https://doi.org/10.1007/s003840050072
8. Yeo SG, Kim MJ, Kim DY, Chang HJ, Kim MJ, Baek JY, Kim SY, Kim TH, Park JW, Oh JH (2013) Patterns of failure in patients with locally advanced rectal cancer receiving pre-operative or post-operative chemoradiotherapy. Radiat Oncol 8:114. https://doi.org/10.1186/1748-717X-8-114
9. Rodel C, Martus P, Papadoupolos T, Fuzesi L, Klimpfinger M, Fietkau R, Liersch T, Hohenberger W, Raab R, Sauer R, Wittekind C (2005) Prognostic significance of tumor regression after preoperative chemoradiotherapy for rectal cancer. J Clin Oncol 23(34):8688–8696. https://doi.org/10.1200/JCO.2005.02.1329
10. Pages F, Berger A, Camus M, Sanchez-Cabo F, Costes A, Molidor R, Mlecnik B, Kirilovsky A, Nilsson M, Damotte D, Meatchi T, Bruneval P, Cugnenc PH, Trajanoski Z, Fridman WH, Galon J (2005) Effector memory T cells, early metastasis, and survival in colorectal cancer. N Engl J Med 353(25):2654–2666. https://doi.org/10.1056/NEJMoa051424
11. Ohtani H (2007) Focus on TILs: prognostic significance of tumor infiltrating lymphocytes in human colorectal cancer. Cancer Immun 7(1):4
12. Huang CY, Chiang SF, Ke TW, Chen TW, You YS, Chen WT, Chao KSC (2018) Clinical significance of programmed death 1 ligand-1 (CD274/PD-L1) and intra-tumoral CD8+ T-cell infiltration in stage II-III colorectal cancer. Sci Rep 8(1):15658. https://doi.org/10.1038/s41598-018-33927-5
13. Rapoport BL, Anderson R (2019) Realizing the Clinical Potential of Immunogenic Cell Death in Cancer Chemotherapy and Radiotherapy. Int J Mol Sci. https://doi.org/10.3390/ijms20040959
14. Huang CY, Chiang SF, Ke TW, Chen TW, Lan YC, You YS, Shiau AC, Chen WT, Chao KSC (2018) Cytosolic high-mobility group box protein 1 (HMGB1) and/or PD-1+ TILs in the tumor microenvironment may be contributing prognostic biomarkers for patients with locally advanced rectal cancer who have undergone neoadjuvant chemoradiotherapy. Cancer Immunol Immunother 67(4):551–562. https://doi.org/10.1007/s00262-017-2109-5
15. Yang F, Zeng Z, Li J, Zheng Y, Wei F, Ren X (2018) PD-1/PD-L1 axis, rather than high-mobility group alarmins or CD8+ tumor-infiltrating lymphocytes, is associated with survival in head and neck squamous cell carcinoma patients who received surgical resection. Front Oncol 8:604. https://doi.org/10.3389/fonc.2018.00604
16. Hernandez C, Huebener P, Schwabe RF (2016) Damage-associated molecular patterns in cancer: a double-edged sword. Oncogene 35(46):5931–5941. https://doi.org/10.1038/onc.2016.104
17. Garg AD, Dudek-Peric AM, Romano E, Agostinis P (2015) Immunogenic cell death. Int J Dev Biol 59(1–3):131–140. https://doi.org/10.1387/ijdb.150061pa
18. Salimu J, Spary LK, Al-Taei S, Clayton A, Mason MD, Staffurth J, Tabi Z (2015) Cross-presentation of the oncofetal tumor antigen 5T4 from irradiated prostate cancer cells–a key role for heat-shock protein 70 and receptor CD91. Cancer Immunol Res 3(6):678–688. https://doi.org/10.1158/2326-6066.CIR-14-0079
19. Medina-Echeverz J, Aranda F, Berraondo P (2014) Myeloid-derived cells are key targets of tumor immunotherapy. Oncoimmunology 3:e28398. https://doi.org/10.4161/onci.28398
20. Vacchelli E, Ma Y, Baracco EE, Zitvogel L, Kroemer G (2016) Yet another pattern recognition receptor involved in the chemotherapy-induced anticancer immune response: formyl peptide receptor-1. Oncoimmunology 5(5):e1118600. https://doi.org/10.1080/2162402X.2015.1118600
21. Baracco EE, Pietrocola F, Buque A, Bloy N, Senovilla L, Zitvogel L, Vacchelli E, Kroemer G (2016) Inhibition of formyl peptide receptor 1 reduces the efficacy of anticancer chemotherapy against carcinogen-induced breast cancer. Oncoimmunology 5(6):e1139275. https://doi.org/10.1080/2162402X.2016.1139275
22. Okazaki S, Loupakis F, Stintzing S, Cao S, Zhang W, Yang D, Ning Y, Sunakawa Y, Stremitzer S, Matsusaka S, Berger MD, Parekh A, West JD, Miyamoto Y, Suenaga M, Schirripa M, Cremolini C, Falcone A, Heinemann V, DePaolo RW, Lenz HJ (2016) Clinical significance of TLR1 I602S polymorphism for patients with metastatic colorectal cancer treated with FOLFIRI plus bevacizumab. Mol Cancer Ther 15(7):1740–1745. https://doi.org/10.1158/1535-7163.MCT-15-0931
23. Vacchelli E, Enot DP, Pietrocola F, Zitvogel L, Kroemer G (2016) Impact of pattern recognition receptors on the prognosis of breast cancer patients undergoing adjuvant chemotherapy. Cancer Res 76(11):3122–3126. https://doi.org/10.1158/0008-5472.CAN-16-0294
24. Vacchelli E, Ma Y, Baracco EE, Sistigu A, Enot DP, Pietrocola F, Yang H, Adjemian S, Chaba K, Semeraro M, Signore M, De Ninno A, Lucarini V, Peschiaroli F, Businaro L, Gerardino A, Manic G, Ulas T, Gunther P, Schultze JL, Kepp O, Stoll G, Lefebvre C, Mulot C, Castoldi F, Rusakiewicz S, Ladoire S, Apetoh L, Bravo-San Pedro JM, Lucattelli M, Delarasse C, Boige V, Ducreux M, Delaloge S, Borg C, Andre F, Schiavoni G, Vitale I, Laurent-Puig P, Mattei F, Zitvogel L, Kroemer G (2015) Chemotherapy-induced antitumor immunity requires formyl peptide receptor 1. Science 350(6263):972–978. https://doi.org/10.1126/science.aad0779
25. Chiang SF, Huang CY, Ke TW, Chen TW, Lan YC, You YS, Chen WT, Chao KSC (2019) Upregulation of tumor PD-L1 by neoadjuvant chemoradiotherapy (neoCRT) confers improved survival in patients with lymph node metastasis of locally advanced rectal cancers. Cancer Immunol Immunother 68(2):283–296. https://doi.org/10.1007/s00262-018-2275-0
26. Wang X, Sheu JJ, Lai MT, Yin-Yi Chang C, Sheng X, Wei L, Gao Y, Wang X, Liu N, Xie W, Chen CM, Ding WY, Sun L (2018) RSF-1 overexpression determines cancer progression and drug resistance in cervical cancer. Biomedicine (Taipei) 8(1):4. https://doi.org/10.1051/bmdcn/2018080104
27. Huang KC, Chiang SF, Chen WT, Chen TW, Hu CH, Yang PC, Ke TW, Chao KSC (2020) Decitabine augments chemotherapy-induced PD-L1 upregulation for PD-L1 blockade in colorectal cancer. Cancers (Basel). https://doi.org/10.3390/cancers12020462
28. Berges C, Naujokat C, Tinapp S, Wieczorek H, Hoh A, Sadeghi M, Opelz G, Daniel V (2005) A cell line model for the differentiation of human dendritic cells. Biochem Biophys Res Commun 333(3):896–907. https://doi.org/10.1016/j.bbrc.2005.05.171
29. Vasconcelos JR, Dominguez MR, Araujo AF, Ersching J, Tararam CA, Bruna-Romero O, Rodrigues MM (2012) Relevance of long-lived CD8(+) T effector memory cells for protective immunity elicited by heterologous prime-boost vaccination. Front Immunol 3:358. https://doi.org/10.3389/fimmu.2012.00358
30. Valujskikh A, Li XC (2007) Frontiers in nephrology: T cell memory as a barrier to transplant tolerance. J Am Soc Nephrol 18(8):2252–2261. https://doi.org/10.1681/ASN.2007020151
31. Retamal-Diaz A, Covian C, Pacheco GA, Castiglione-Matamala AT, Bueno SM, Gonzalez PA, Kalergis AM (2019) Contribution of resident memory CD8(+) T cells to protective immunity against respiratory syncytial virus and their impact on vaccine design. Pathogens 8(3):147. https://doi.org/10.3390/pathogens8030147
32. Krombach J, Hennel R, Brix N, Orth M, Schoetz U, Ernst A, Schuster J, Zuchtriegel G, Reichel CA, Bierschenk S, Sperandio M, Vogl T, Unkel S, Belka C, Lauber K (2019) Priming anti-tumor immunity by radiotherapy: dying tumor cell-derived DAMPs trigger endothelial cell activation and recruitment of myeloid cells.

Oncoimmunology 8(1):e1523097. https://doi.org/10.1080/2162402X.2018.1523097
33. Vecchi L, Zóia MAP, Santos TG, de Oliveira Beserra A, Colaço Ramos CM, Matias Colombo BF, Paiva Maia YC, Piana de Andrade V, Soares Mota ST, Gonçalves de Araújo T, Van Petten de Vasconcelos Azevedo F, Soares FA, Oliani SM, Goulart LR (2018) Inhibition of the AnxA1/FPR1 autocrine axis reduces MDA-MB-231 breast cancer cell growth and aggressiveness in vitro and in vivo. Biochim Biophys Acta (BBA) Mol Cell Res 1865 (9):1368-1382. https://doi.org/10.1016/j.bbamcr.2018.06.010
34. Gray V, Briggs S, Palles C, Jaeger E, Iveson T, Kerr R, Saunders MP, Paul J, Harkin A, McQueen J, Summers MG, Johnstone E, Wang H, Gatcombe L, Maughan TS, Kaplan R, Escott-Price V, Al-Tassan NA, Meyer BF, Wakil SM, Houlston RS, Cheadle JP, Tomlinson I, Church DN (2019) Pattern recognition receptor polymorphisms as predictors of oxaliplatin benefit in colorectal cancer. J Natl Cancer Inst. https://doi.org/10.1093/jnci/djy215
35. Demaria S, Golden EB, Formenti SC (2015) Role of local radiation therapy in cancer immunotherapy. JAMA Oncol 1(9):1325. https://doi.org/10.1001/jamaoncol.2015.2756
36. Honda M, Takeichi T, Hashimoto S, Yoshii D, Isono K, Hayashida S, Ohya Y, Yamamoto H, Sugawara Y, Inomata Y (2017) Intravital Imaging of Neutrophil Recruitment Reveals the Efficacy of FPR1 Blockade in Hepatic Ischemia-Reperfusion Injury. J Immunol 198(4):1718–1728. https://doi.org/10.4049/jimmunol.1601773
37. Yang D, Chen Q, Le Y, Wang JM, Oppenheim JJ (2001) Differential regulation of formyl peptide receptor-like 1 expression during the differentiation of monocytes to dendritic cells and macrophages. J Immunol 166(6):4092–4098
38. Wenzel-Seifert K, Seifert R (2003) Functional differences between human formyl peptide receptor isoforms 26, 98, and G6. Naunyn Schmiedebergs Arch Pharmacol 367(5):509–515. https://doi.org/10.1007/s00210-003-0714-7
39. Lee HY, Jeong YS, Lee M, Kweon HS, Huh YH, Park JS, Hwang JE, Kim K, Bae YS (2018) Intracellular formyl peptide receptor regulates naive CD4 T cell migration. Biochem Biophys Res Commun 497(1):226–232. https://doi.org/10.1016/j.bbrc.2018.02.060